Elsholtzia communis leaf extract mediated synthesis of silver nanoparticles: enhanced antioxidant, antidiabetic and antiproliferative activity

S. Begum[a], K. D. Chanu[b], N. Sharma[b], R. K. L. Singh[c,*]
[a]*Department of Chemistry, Manipur University, Canchipur, Manipur, India*
[b]*Institute of Bio-resources and Sustainable Development (IBSD), Takyelpat, Manipur, India*
[c]*Department of Chemistry, Dhanamanjuri University, Manipur, India*

Nanoparticles of silver were synthesised utilising water leaf extract of *Elsholtzia communis* (Collett and Hemsl.) Diels (ECO). The formation of *Elsholtzia communis* silver nanoparticles (ECO-AgNPs) was monitored by a UV-visible spectrophotometer. From the TEM and XRD analysis, the average particle and crystallite size of ECO-AgNPs was determined as 11.38 nm and 8.52 nm, respectively. DLS studies of ECO-AgNPs showed the ζ-potential value of −59.4 mV and a polydispersity index (PDI) of 0.149. The phytochemicals responsible for the reduction of silver ions were confirmed through FTIR spectroscopy and further supported by HRLC-MS analysis. Dose-dependent antioxidant and antidiabetic activities were demonstrated by the biosynthesized nanoparticles. The antiproliferative activity of ECO-AgNPs was estimated using 3-(4,5-dimethylthiazol-2-yl)-2,5-diphenyltetrazolium bromide (MTT) assay on HeLa, HCT 116 and A549 cell lines and their IC_{50} values were found to be 71.33 ± 2.89 µg/mL, 33.45 ± 0.21 µg/mL, and 28.91 ± 5.01 µg/mL, respectively. The results showed that *Elsholtzia communis* AgNPs have enhanced antiproliferative, antioxidant, and antidiabetic activities and may be employed as beneficial nanocompounds.

(Received November 15, 2023; February 2, 2024)

Keywords: Silver nanoparticles, *Elsholtzia communis*, Antioxidant, Antidiabetic, Antiproliferative

1. Introduction

Nanoparticles are sets of substances where at least one dimension is less than approximately 100 nm [1,2]. Nanoparticles have found widespread application in nanotechnological devices and the biomedical area due to their high surface-volume ratio and increased physical, chemical, and biological effects compared to their macroscopic counterparts [3]. Metal nanoparticles, particularly silver nanoparticles, are extremely important because of their applications in biological and medical research [4]. Numerous hazardous substances are involved in the chemical and physical synthesis of nanoparticles. As an alternative, the synthesis of metal nanoparticles using plant extracts is becoming increasingly appealing because it is less expensive, more environmentally friendly, and takes less time. Silver nanoparticles were fabricated using leaf extracts from *Averrhoa bilimbi* [5], *Callisia fragrans* [6], *Punica granatum* [7], and *Acer oblongifolium* [8]. Many species of *Elsholtzia* have shown antioxidant, antidiabetic and antiproliferative activities [9,10]. *Elsholtzia communis* (Collett and Hemsl.) Diels var. purple flower (family: *Lamiaceae*) is available in Manipur, India, and its polyphenolic compounds and free radical scavenging capacity have been reported [11]. Because of the presence of medicinal properties in many *Elsholtzia* species, it is our strong belief that the biosynthesised silver nanoparticles using *Elsholtzia communis* will have enhanced effects on antioxidant, antidiabetic, and antiproliferative properties. This work explained the synthesis of silver nanoparticles using aqueous leaf extract of *Elsholtzia communis* and highlighted the enhanced antioxidant, antidiabetic, and antiproliferative effects against cancer cell lines.

* Corresponding author: london_ningthemcha@yahoo.com
https://doi.org/10.15251/DJNB.2024.191.251

2. Experimental

2.1. *Materials*

Silver nitrate ($AgNO_3$), 2,2′-azino-bis (3-ethylbenzothiazoline-6-sulfonic acid) (ABTS), 2,2-diphenyl-1-picrylhydrazyl (DPPH), 3-(4,5-dimethylthiazol-2-yl)-2,5-diphenyltetrazolium bromide (MTT), α-glucosidase, α-amylase, 4-nitro-phenyl-α-D-glucopyranoside (pNPG), acarbose, and other chemicals were obtained from Sigma-Aldrich and renowned companies. Milli-Q water was used to prepare the solutions.

2.2. *Plant extract preparation and synthesis of ECO-AgNPs*

Fresh leaves of ECO were collected from the local markets of Imphal, Manipur, India, and cleaned using distilled water. An electric grinder was used to powder dried leaves. Ten grams of powdered leaf with 200 mL of deionized water was heated at 60 °C for 10 min, filtered to obtain the aqueous ECO leaf extract, and stored at 4 °C for further use. Aqueous ECO leaf extract (20 mL) was mixed with 200 mL of silver nitrate (10 mM) solution and heated at 70 °C for 25 min to obtain ECO-AgNPs. The progress of nanoparticle formation was monitored by observing the UV-visible spectra of the mixture every 5 min for a total duration of 50 min. The synthesized ECO-AgNPs were collected by centrifugation using a REMI Centrifuge R24 (10000 rpm, 15 min) and cleaned three times with deionized water, dried at 45 °C, and stored for characterization.

2.3. Characterisation of ECO-AgNPs

Shimadzu UV-1900i spectrophotometer with a wavelength range of 350-800 nm was used for recording absorption spectra of the synthesised ECO-AgNPs at room temperature. The PDI and ζ-potential of the ECO-AgNPs were estimated by zeta sizer (Nano ZS90, Malvern Instrument). The particle size of the ECO-AgNPs was determined by HR-TEM (JEOL JEM-2100). Field-emission scanning electron microscopy (MAGNA TESCAN) combined with Energy Dispersive X-ray Spectroscopy (EDX) was employed to examine the surface morphology and chemical composition of the ECO-AgNPs. The XRD diffractogram of the silver nanoparticles was measured using a BRUKER-D8 Advanced diffractometer with Cu Kα radiation (λ = 1.54 Å) within the 2θ range 20-80°. An FTIR spectrometer (Perkin Elmer, Spectrum 2) scanning in the range of 450-4000 cm^{-1} was used to analyse phytochemicals that reduced silver ions and stabilizing ECO-AgNPs.

2.4. Phytochemical analysis by HRLC-MS

The phytochemicals analysis was carried out using a Thermo Scientific Q Exactive Orbitrap mass spectrometer (Thermo Fisher Scientific, Waltham, MA, USA) coupled to Dionex UltiMate 3000 ultra-high-performance liquid chromatography system (Thermo Fisher Scientific, Waltham, MA, USA) with Hypersil Gold C18 column (2.1 mm × 100 mm, 1.9 μm). Throughout the analysis, the column was maintained at 40 °C at a flow rate of 300 μL/min. HPLC-grade deionized water containing 0.1% formic acid (Buffer A) and a mixture of 0.1% formic acid in 90% acetonitrile with 10% deionized water (Buffer B) were used as the mobile phase. The settings of the mass spectrometer were as follows: Scan Range = 120-1200 m/z, resolution = 70,000, Automatic Gain Control (AGC) = 1e6, Sheath Gas flow rate = 30 (a.u), Auxiliary Gas flow rate = 10 (a.u), Capillary Voltage = (+) 3.5 kV, Capillary Temperature = 275 °C, S-Lens RF Level = 50, and Probe Heater Temperature = 320 °C. Scanning was performed in the full MS mode. The data obtained were analyzed and processed using Thermo Fisher Scientific (Waltham, MA, USA) Compound Discoverer 3.3 software.

2.5. Antioxidant activities

2.5.1. DPPH radical scavenging assay

The antioxidant capacities of ECO and ECO-AgNPs were analyzed by slight modifications of the method of Yong et al. [12]. A 100 μL of ECO-AgNPs at various concentrations (5, 7, 10, 15, 20, 25, 30, 40 μg/mL) and 100 μL of DPPH (0.2 mM in methanol) were mixed and agitated before incubation in the dark for 30 min and recorded absorbance at 517 nm using a Varioskan LUX multimode microplate reader (ESW version 1.00.38). All experiments were performed in triplicate

using l-ascorbic acid as the standard. The above procedure was repeated using the ECO leaf extract. The DPPH free radical-scavenging capacity (%) was calculated using Equation (1):

$$\text{DPPH scavenging capacity (\%)} = \left(\frac{\text{Abs of control} - \text{Abs of sample}}{\text{Abs of control}}\right) \times 100 \quad (1)$$

2.5.2. ABTS radical scavenging assay

The ABTS scavenging activities of ECO and ECO-AgNPs were estimated following the slight modifications of Khan et al. [13]. ABTS solution was prepared by mixing 7.4 mM ABTS and 2.6 mM potassium persulfate. A 100 µL of ABTS solution was mixed with 100 µL of ECO-AgNPs at concentrations of 5, 7, 10, 15, 20, 25, and 30 µg/mL. The same procedure was repeated for the ECO leaf extract. All experiments were performed three times with l-ascorbic acid as the standard. Absorbance at 734 nm was recorded using a Varioskan LUX multimode microplate reader. ABTS scavenging capacity was measured using equation (2):

$$\text{ABTS scavenging capacity (\%)} = \left(\frac{\text{Abs of control} - \text{Abs of sample}}{\text{Abs of control}}\right) \times 100 \quad (2)$$

2.6. Antidiabetic activities

2.6.1. α-Glucosidase inhibition activity of ECO-AgNPs

To test the inhibition of α-glucosidase, a modified method was adopted [14]. A 150 µL assay mixture consisting of 0.1 M sodium phosphate buffer (pH 6.9, 6 mM NaCl), with different concentrations of ECO-AgNPs (20, 40, 50, 60, 70, 80, 100 & 120 µg/mL) and α-glucosidase (0.1 units) was incubated for 10 min at 37° C. The mixture was then incubated again for 20 min at 37 °C with 50 µL (2 mM) p-nitrophenyl-α-d-glucopyranoside (pNPG) in sodium phosphate buffer. A Thermo Fisher Scientific Varioskan LUX multimode microplate reader (ESW version 1.00.38) was used to measure the absorbance at 405 nm after it was stopped by injecting 50 µL of 0.1 M sodium carbonate (Na_2CO_3). The above procedures were also followed for the ECO leaf extract. Acarbose served as the positive control, whereas the tube containing 100% α-glucosidase activity, but without ECO-AgNPs, served as the control. The percentage inhibition (% I) was evaluated using formula (3).

$$\%\ \text{I} = \left(1 - \frac{\text{A}}{\text{B}}\right) \times 100 \quad (3)$$

where A is the absorbance in the presence of the sample, and B is the absorbance in the presence of phosphate buffer (control).

2.6.2. α-Amylase inhibition assay of ECO-AgNPs

The usual procedure with a few minor modifications was used to perform the α-amylase inhibition experiments [15]. In a 96-well microplate, a reaction mixture consisting of 20 µL of different concentrations of ECO-AgNPs (20, 40, 50, 60, 70, 80, 100, and 120 µg/mL), 10 µL α-amylase (2 U/mL), 50 µL phosphate buffer (100 mM, pH 6.8), and standard (acarbose) was added and incubated for 20 min at 37 °C, and then 10 µL of 1% soluble starch was added. The reaction mixture was then incubated for 30 min. A colour reagent DNS (100 µL) was introduced to stop the reaction and boiled at 95 °C for 15 min, followed by measurement of the absorbance at 450 nm using a multi-plate reader. The mean of the three independent observations was taken as the result, and percentage inhibition (% I) was calculated using the following relation (4):

$$\%\ \text{I} = \left(1 - \frac{\text{A}}{\text{B}}\right) \times 100 \quad (4)$$

where A is the absorbance in the presence of the sample, and B is the absorbance in the presence of phosphate buffer (control).

2.7. Antiproliferative activity

The MTT viability assay was performed according to the protocol described by Pungle's co-workers' protocol [16]. In a 96-well plate, 5×10^3 cells were plated in a humidified 5% CO_2 cell culture incubator and incubated at 37 °C for 24 h. Before administering the treatment, ECO-AgNPs were dissolved in 10% DMSO stock solution and then diluted with growth media to concentrations of 3, 6, 12, 25, 50, 100, and 200 µg/mL. Different concentrations of ECO-AgNPs were mixed with cells and incubated for 48 h. In each well, 15 µL of MTT reagent (5 mg/mL in PBS) was added and the cells were incubated for 3 h. DMSO (100 µL) was added after the incubation and thoroughly mixed to dissolve the product. A Varioskan LUX multimode microplate reader ESW version 1.00.38; Thermo Fisher Scientific was used to measure absorbance at 570 nm. Cells in culture media were used as a negative control. Cell viability (%) was calculated using Equation (5):

$$\% \text{ cell viability} = \left(\frac{\text{Mean Abs of sample}}{\text{Mean Abs of control}}\right) \times 100 \quad (5)$$

3. Results and discussion

3.1. Silver nanoparticles characterisation

UV-vis absorbance spectral analysis of AgNPs resulted in a single maximum absorbance peak at 449 nm, which is a characteristic SPR band of AgNPs and authenticated the formation of ECO-AgNPs [17]. After 10 min, the formation of ECO-AgNPs began and was completed after 50 min (figure 1).

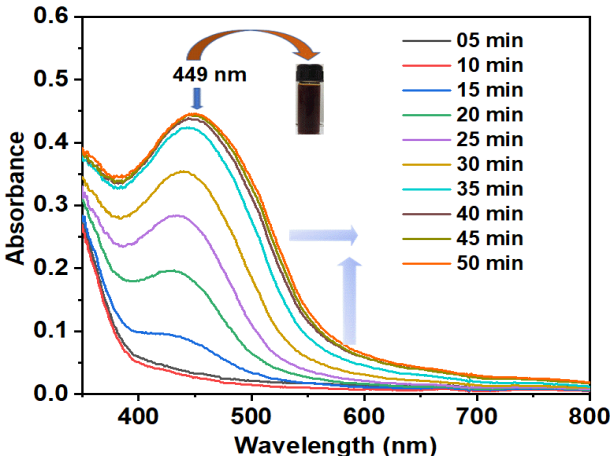

Fig. 1. UV-vis spectra of ECO-AgNPs at various time intervals.

The XRD pattern shown in figure 2 confirms the crystallinity of the ECO-AgNPs. Four prominent peaks at 2θ values of 38.100° (111), 43.900° (200), 64.499° (220), and 77.268° (311) were validated using XRD and ascribed to the silver fcc structure of JCPDS File No. 04-0783 well. Other peaks were observed in addition to the above peaks at 28.01° and 32.13°, which may be a result of the chemical components in the leaf extract that reduce silver ions and stabilize the resulting nanoparticles [18,19]. Using the Debye-Scherrer equation, $D = K\lambda/(\beta\cos\theta)$, where, K = 0.94 is the Scherrer constant, λ (0.154 nm) is the X-ray wavelength, β (radian) is fullwidth at half maximum (FWHM) of the XRD peaks, the average crystallite size was calculated as 8.52 nm [20].

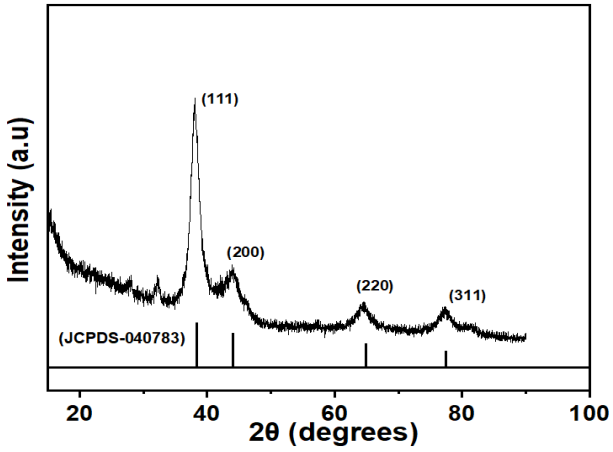

Fig. 2. XRD pattern of ECO-AgNPs.

Phytochemicals in the plant extract that reduced silver ions to AgNPs were identified by FTIR spectroscopy. Figure 3a and figure 3b show the FTIR spectra of the ECO leaf extract and ECO-AgNPs, respectively. FTIR spectrum of ECO leaf extract showed peaks at 876, 1044, 1086, 1639, 2980 and 3340 cm^{-1}. The FTIR spectrum of ECO-AgNPs showed absorption peaks at 1638 and 3339 cm^{-1} due to the presence of carbonyl and phenolic compounds respectively [21]. The strong broad absorption band at 3340 cm^{-1} is assigned to O-H stretching vibration in alcohols and phenolic compounds [22]. The peak at 2980 cm^{-1} is attributed to O-H stretch in alcohols [23]. Absorption at 1044 cm^{-1} is ascribed to the O-H stretching of the phenol group. The peaks at 876 cm^{-1} and 1086 cm^{-1} are attributed to C-C and C-O stretching respectively [24]. FTIR spectrum of ECO-AgNPs shows the disappearance of peaks at 876, 1044, 1086 and 2980 cm^{-1} and slight shifting of peaks at 1638 and 3339 cm^{-1} indicating the dual role of ECO leaf extract as a reducing agent and as a stabilising agent as well [25].

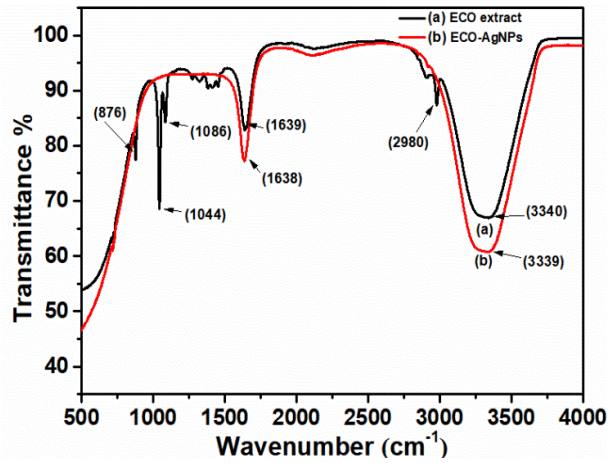

Fig. 3. FTIR spectra. (a) ECO leaf extract and (b) ECO-AgNPs.

Silver nanoparticles of spherical shape with a particle size of 11.38 nm were evident from TEM images (figure 4a). The SAED patterns of ECO-AgNPs are shown in figure 4b, and they correspond to the planes (111), (200), (220), and (311), and are compatible with the XRD pattern. Figure 4c shows a lattice fringe of 0.225 nm whereas the particle size distribution of ECO-AgNPs is shown in figure 4d.

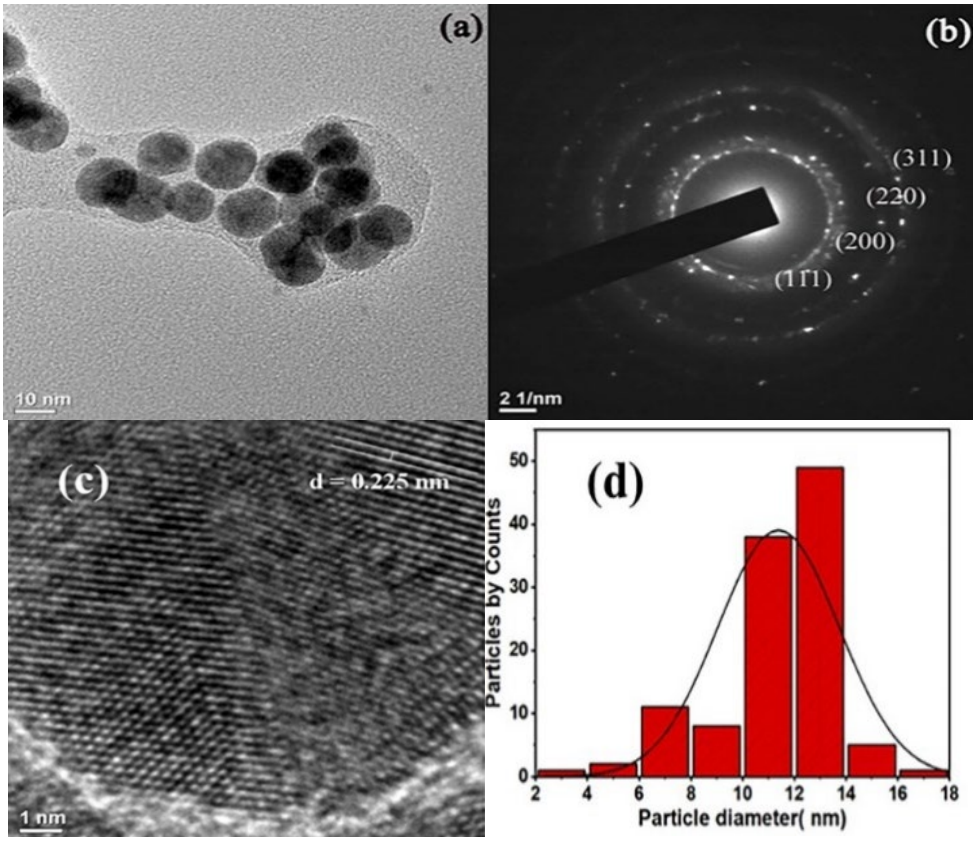

Fig. 4. ECO-AgNPs. (a) TEM image, (b) SAED pattern, (c) Lattice fringes with d-spacing and (d) Particle size distribution.

FESEM images of ECO-AgNPs are shown in figure 5a and are nearly spherical with a slight agglomeration of the nanoparticles. The capping agent of plant biomolecules binding with AgNPs may cause particle aggregation [26–28]. The EDS spectra of the silver nanoparticles are displayed in figure 5b and the presence of elemental metal silver (98.93%) was confirmed. The EDS profile displays a strong silver signal with an oxygen peak that might have originated from the biomolecules attached to the silver.

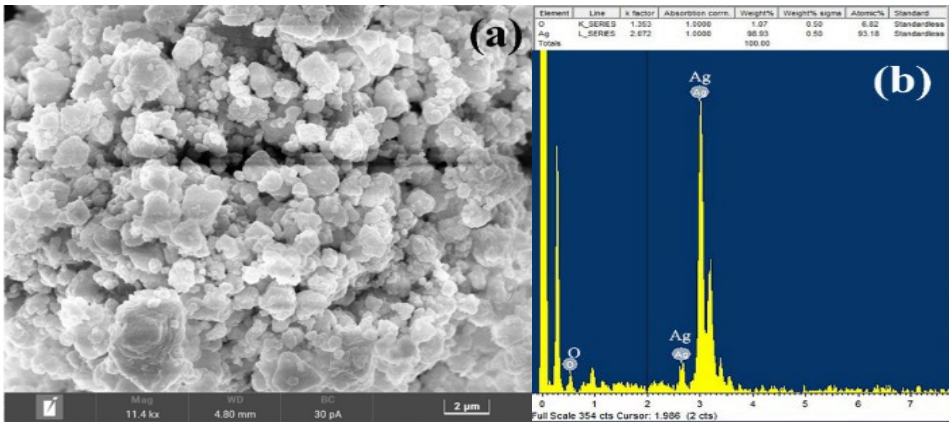

Fig. 5. ECO-AgNPs. (a) FESEM and (b) EDS spectra.

Figure 6a and figure 6b show the ζ-potential of -59.4 mV and average particle size (hydrodynamic) distribution of 125.4 nm respectively. The PDI value of ECO-AgNPs was found to be 0.149 which is less than 1 attributes the presence of monodisperse nanoparticles. The hydration layer on the nanoparticles' surface is responsible for the larger size obtained from the DLS than the size inferred through the TEM images [22]. ECO-AgNPs have a negative ζ-potential value due to the presence of negatively charged functional groups in the plant extract, which contributes to their stability [29].

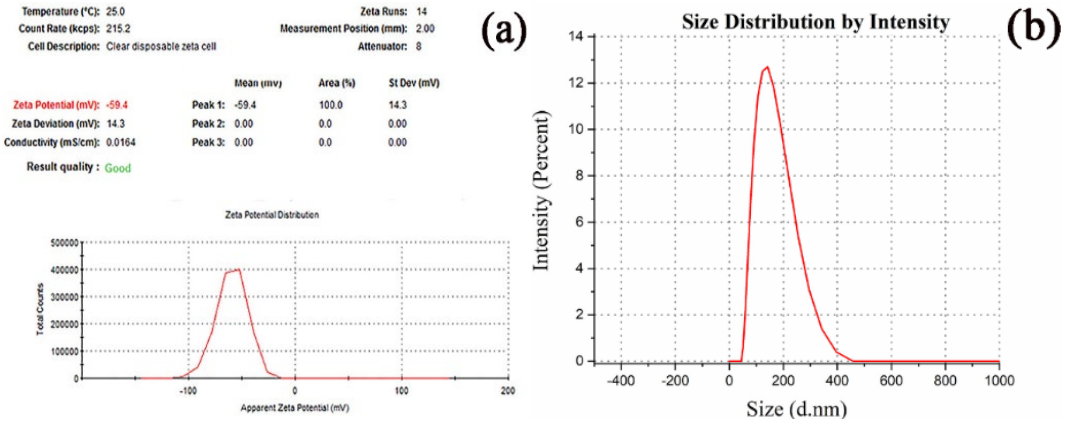

Fig. 6. DLS spectra of ECO-AgNPs. (a) ζ−potential and (b) size distribution.

3.2. Phytochemical profiling of aqueous leaf extract of ECO

The phytochemicals present in the aqueous leaf extract of ECO were confirmed by HRLC-MS analysis. In this analysis, the phytochemicals were segregated and verified depending on their molecular weight, molecular formula, retention time (RT), m/z and area [30]. The HRLC-MS spectrogram of ECO is shown in figure 7. The ten most abundant phenolic compounds present in the plant extract are shown in table 1.

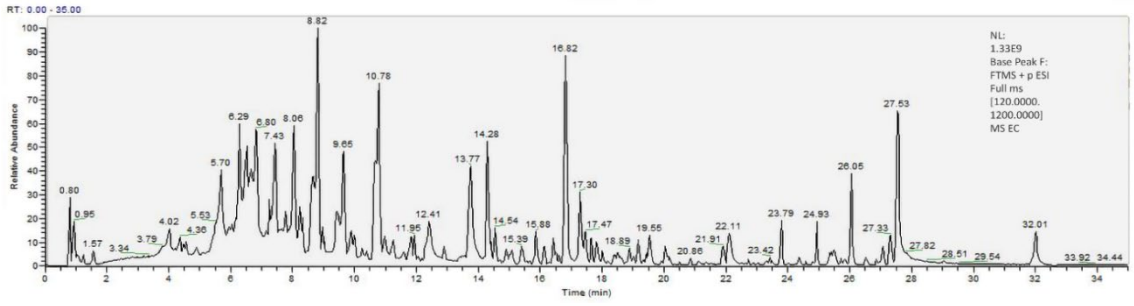

Fig. 7. HRLC-MS analysis of the ECO spectrum.

Table 1. Ten most abundant phenolic compounds found in ECO leaf extract.

Sl. No.	Compound	Molecular Formula	Molecular Weight	m/z	Retention time (min)	Area	Intensity (Count) (10^6)
1.	Genistin	C21H20O10	432.10548	433.11276	8.048	6160502310	800
2.	Luteolin	C15H10O6	286.04756	287.05484	9.637	4612464682	660
3.	Caffeic acid	C9H8O4	180.04218	163.03889	8.231	2288362214	340
4.	Aspirin	C9H8O4	180.04221	163.03889	5.081	1136034072	45
5.	Apigenin	C15H10O5	270.05159	271.05887	8.048	575136955.4	65
6.	(+/-)-Rosmarinic acid	C18H16O8	360.08419	361.0914	8.231	295032380	48
7.	Kaempferol	C15H10O6	286.0464	287.05368	7.254	270396207.5	30
8.	Quercetin	C15H10O7	302.04219	303.04947	7.145	264832380.7	46
9.	Tiliroside	C30H26O13	594.13713	595.14441	9.736	141588150.7	22
10.	(-)-Shikimic acid	C7H10O5	174.05284	157.04955	3.441	110515844.3	4.5

3.3. Antioxidant activity

DPPH and ABTS assays measured the in vitro antioxidant activity of ECO-AgNPs and the aqueous leaf extract of ECO. It can be inferred from the analysis that the aqueous ECO leaf extract and ECO-AgNPs boosted the scavenging action on DPPH (figure 8a) and ABTS radicals (figure 8b) in a dose-response manner, and employed ascorbic acid as a reference. The obtained results indicated that IC_{50} values on both assays of ECO-AgNPs (9.21 ± 0.26 and 5.24 ± 0.23 µg/mL), ascorbic acid (32.76 ± 1.24 and 14.85 ± 0.22 µg/mL), and ECO leaf extract (24.77 ± 0.46 and 19.81 ± 0.20 µg/mL) respectively (table 2) and concluded that ECO-AgNPs inhibited remarkably than the standard and aqueous ECO leaf extract. Functional groups attached to ECO-AgNPs that were derived from the plant extract may be responsible for their antioxidant properties [31,32].

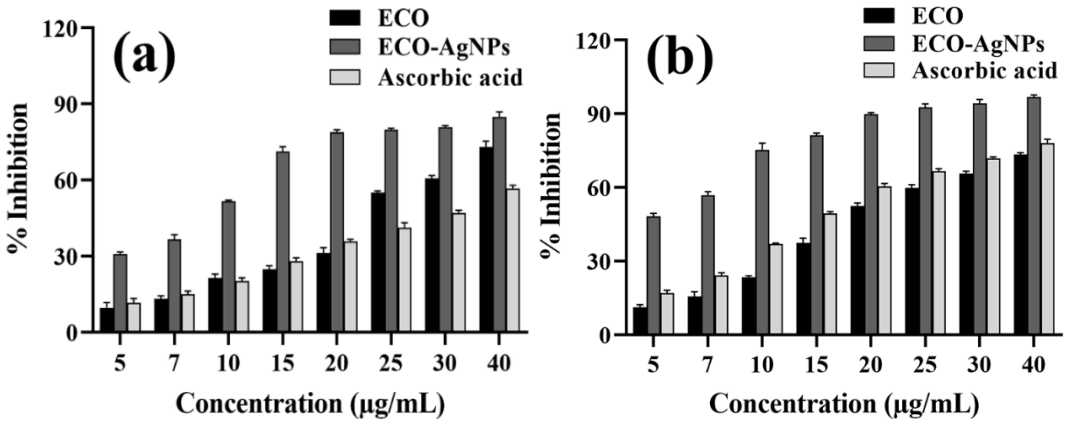

Fig. 8. Scavenging activities of ECO-AgNPs and ECO. (a) DPPH and (b) ABTS.

Table 2. Scavenging activities of ECO-AgNPS and ECO leaf extract.

Antioxidant Assay	IC_{50} (µg/mL)		
	ECO	ECO-AgNPs	Ascorbic acid
DPPH	24.77 ± 0.46	9.21 ± 0.26	32.76 ± 1.24
ABTS	19.81 ± 0.20	5.24 ± 0.23	14.85 ± 0.22

3.4. Antidiabetic activity

An essential strategy to avoid the rise in blood glucose levels is the suppression of the enzymes responsible for digesting carbohydrates namely α-glucosidase and α-amylase [33]. The ECO-AgNPs have inhibited α-glucosidase (figure 9a) and α-amylase (figure 9b) activities potentially in a substantial dose-dependent manner. The IC_{50} values of ECO-AgNPs on α-glucosidase and α-amylase are 26.87 ± 1.74 µg/mL and 40.6 ± 1.77 µg/mL, respectively. The IC_{50} values of ECO leaf extract against the α-glucosidase and α-amylase were found to be 37.45 ± 0.95 µg/mL and 55.78 ± 0.20 µg/mL respectively whereas, IC_{50} of standard (acarbose) against α-glucosidase and α-amylase were 51.46 ± 2.38 µg/mL and 65.7 ± 0.40 µg/mL respectively. All these IC_{50} values are shown in table 3. From these studies, it can be observed that ECO-AgNPs significantly show synergistic inhibition activity against α- glucosidase and α- amylase than the ECO leaf extract and standard.

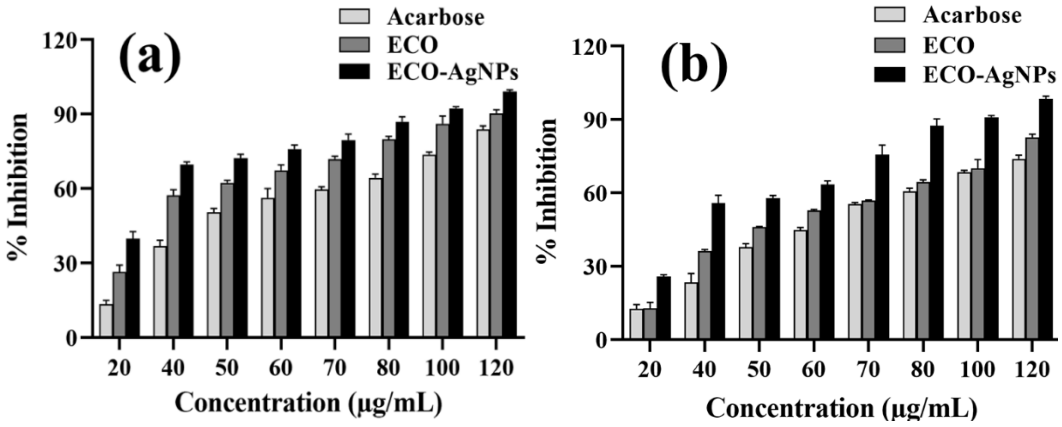

Fig. 9. Effect of ECO-AgNPs and ECO (a) α-glucosidase and (b) α-amylase.

Table 3. The antidiabetic activities of ECO-AgNPS and ECO leaf extract.

Enzyme Assay	IC_{50} (µg/mL)		
	ECO	ECO-AgNPs	Acarbose
α-glucosidase	37.45 ± 0.95	26.87 ± 1.74	51.46 ± 2.38
α-amylase	55.78 ± 0.20	40.6 ± 1.77	65.7 ± 0.40

3.5. ECO-AgNPs induce cytotoxic activity on cancer cell lines

MTT assays for antiproliferation activity were applied against the cancer cell lines HeLa, A549 and HCT116 with the synthesized ECO-AgNPs at various concentrations. Cell cytotoxicity increased with increasing concentration of ECO-AgNPs after 48 h of treatment. Figure 10a shows the highest antiproliferative effects of ECO-AgNPs against A549 as compared to the HeLa cell line and HCT 116. Table 4 shows the IC_{50} values of ECO-AgNPs against A549 (IC_{50} = 28.91 ± 5.01 µg/mL), HeLa cell line (IC_{50} = 71.33 ± 2.89 µg/mL) and HCT 116 (IC_{50} = 33.45 ± 0.21 µg/mL). The poor antiproliferative effect of ECO leaf extract can be seen in figure 10b. Reproduced data are

Mean ± SD of three distinct experiments. These results affirmed that ECO-AgNPs show synergistic antiproliferative activities against HeLa, A549, HCT 116 cell lines [34].

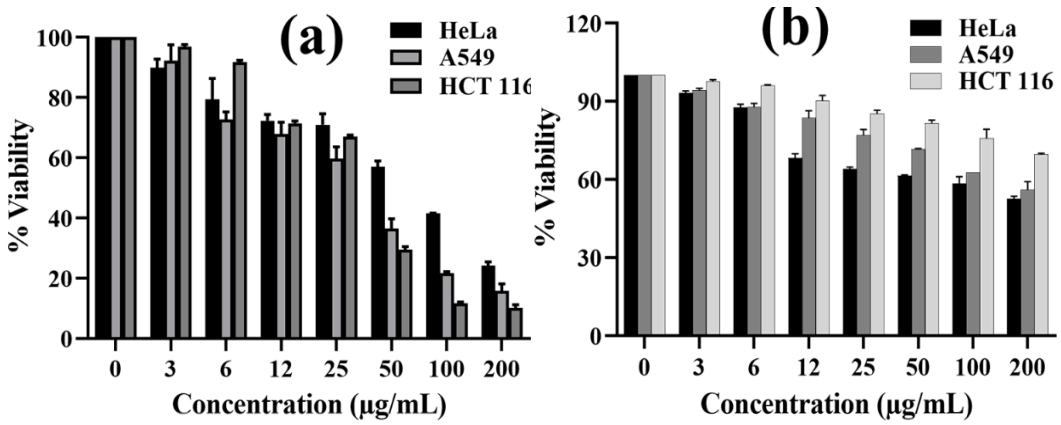

Fig. 10. Cytotoxic effects on cancer cell lines (a) ECO-AgNPs and (b) ECO.

Table 4. The antiproliferative activities of ECO-AgNPS.

Cell Line	IC_{50}
HeLa	71.33 ± 2.89 µg/mL
A549	28.91 ± 5.01 µg/mL
HCT116	33.45 ± 0.21 µg/mL

4. Conclusion

Using aqueous ECO leaf extract, spherical silver nanoparticles were synthesised. The reduction of silver ions and stabilisation of silver nanoparticles were triggered by the phytochemicals present in the leaf extract. The biosynthesized ECO-AgNPs have shown enhanced antioxidant, antidiabetic and antiproliferative activities. Amongst the antiproliferative properties of ECO-AgNPs against the cell lines HeLa, A549, and HCT 116, A549 is the most effective. The biosynthesised ECO-AgNPs may result in the output of more efficient antiproliferative, antidiabetic and antioxidant drugs in the pharmaceutical industry.

Acknowledgements

The authors are very appreciative of the technical support given by the Sophisticated Analytical Instrument Facility (SAIF) at Shillong and the National Institute of Technology (NIT), Imphal, India, in characterising the ECO-AgNPs.

References

[1] N. Baig, I. Kammakakam and W. Falath, Mater. Adv. 2, 1821 (2021); https://doi.org/10.1039/D0MA00807A

[2] I. Khan, K. Saeed and I. Khan, Arabian Journal of Chemistry. 12, 908 (2019); https://doi.org/10.1016/j.arabjc.2017.05.011

[3] Hemlata, P. R. Meena, A. P. Singh, and K. K. Tejavath, ACS Omega. 5, 10 (2020); https://doi.org/10.1021/acsomega.0c00155

[4] H. A. Widatalla, L. F. Yassin, A. A. Alrasheid, S. A. Rahman Ahmed and M. O. Widdatallah, Nanoscale Advances. 4, 911 (2022); https://doi.org/10.1039/D1NA00509J

[5] L. V. Hublikar, S. V. Ganachari and V. B. Patil, Nanoscale Adv. 5, 4149 (2023); https://doi.org/10.1039/D3NA00313B

[6] L. A. T. Nguyen, B. Van Mai, D. Van Nguyen, N. Q. T. Nguyen, V. Van Pham, T. L. M. Pham and H. T. Le, Green Processing and Synthesis. 12, 20230024 (2023); https://doi.org/10.1515/gps-2023-0024

[7] S. Sarkar and V. Kotteeswaran, Adv. Nat. Sci: Nanosci. Nanotechnol. 9, 025014 (2018); https://doi.org/10.1088/2043-6254/aac590

[8] M. Naveed et al., Molecules. 27, 4226 (2022); https://doi.org/10.3390/molecules27134226

[9] S. Begum, K. D. Chanu, N. Sharma and R. K. London Singh, Asian J. Chem. 35, 732 (2023); https://doi.org/10.14233/ajchem.2023.27583

[10] Z. Guo, Z. Liu, X. Wang, W. Liu, R. Jiang, R. Cheng and G. She, Chem Cent J. 6, 147 (2012); https://doi.org/10.1186/1752-153X-6-147

[11] S. D. Khomdram and P. K. Singh, Not Sci Biol. 3, 108 (2011); https://doi.org/10.15835/nsb325638

[12] Y. K. Yong, J. J. Tan, S. S. Teh, S. H. Mah, G. C. L. Ee, H. S. Chiong and Z. Ahmad, Clinacanthus Nutans Evidence-Based Complementary and Alternative Medicine. 2013, e462751 (2013); https://doi.org/10.1155/2013/462751

[13] R. A. Khan, M. R. Khan, S. Sahreen and M. Ahmed, Chemistry Central Journal. 6, 12 (2012); https://doi.org/10.1186/1752-153X-6-43

[14] N. G. E. R. Etsassala, J. A. Badmus, J. L. Marnewick, E. I. Iwuoha, F. Nchu and A. A. Hussein, Antioxidants. 9, 1149 (2020); https://doi.org/10.3390/antiox9111149

[15] B. M. I. S. Jadalla, J. J. Moser, R. Sharma, N. G. E. R. Etsassala, S. A. Egieyeh, J. A. Badmus, J. L. Marnewick, D. Beukes, C. N. Cupido and A. A. Hussein, Separations. 9, 190 (2022); https://doi.org/10.3390/separations9080190

[16] R. Pungle, S. H. Nile, N. Makwana, R. Singh, R. P. Singh and A. S. Kharat, Oxidative Medicine and Cellular Longevity. 2022, 1 (2022); https://doi.org/10.1155/2022/9671594

[17] H. M. M. Ibrahim, Journal of Radiation Research and Applied Sciences. 8, 265 (2015); https://doi.org/10.1016/j.jrras.2015.01.007

[18] R. Kumar, S. M. Roopan, A. Prabhakarn, V. G. Khanna and S. Chakroborty, Spectrochimica Acta Part A: Molecular and Biomolecular Spectroscopy. 90, 173 (2012); https://doi.org/10.1016/j.saa.2012.01.029

[19] S. M. Roopan, Rohit, G. Madhumitha, A. A. Rahuman, C. Kamaraj, A. Bharathi and T. V. Surendra, Industrial Crops and Products. 43, 631 (2013); https://doi.org/10.1016/j.indcrop.2012.08.013

[20] A. L. Patterson, Physical Review. 56, 978 (1939); https://doi.org/10.1103/PhysRev.56.978

[21] S. Sarkar and V. Kotteeswaran, Adv. Nat. Sci: Nanosci. Nanotechnol. 9, 025014 (2018); https://doi.org/10.1088/2043-6254/aac590

[22] G. Singhal, R. Bhavesh, K. Kasariya, A. R. Sharma and R. P. Singh, J Nanopart Res. 13, 2981 (2011); https://doi.org/10.1007/s11051-010-0193-y

[23] S. Wu, S. Rajeshkumar, M. Madasamy and V. Mahendran, Artificial Cells, Nanomedicine, and Biotechnology. 48, 1153 (2020); https://doi.org/10.1080/21691401.2020.1817053

[24] W. Suvandee, V. Teeranachaideekul, N. Jeenduang, P. Nooeaid, A. Makarasen, L. Chuenchom, S. Techasakul and D. Dechtrirat, Polymers. 14, 2205 (2022); https://doi.org/10.3390/polym14112205

[25] M. Ismail, S. Gul, M. I. Khan, M. A. Khan, A. M. Asiri and S. B. Khan, Green Processing and Synthesis 8, 118 (2019); https://doi.org/10.1515/gps-2018-0030

[26] A. A. Fairuzi, N. N. Bonnia, R. M. Akhir, M. A. Abrani and H. M. Akil, IOP Conference Series: Earth and Environmental Science 105, 0 (2018); https://doi.org/10.1088/1755-1315/105/1/012018

[27] S. Raj, H. Singh, R. Trivedi, and V. Soni, Sci Rep. 10(1), 9616 (2020); https://doi.org/10.1038/s41598-020-66851-8

[28] M. Vanaja, K. Paulkumar, M. Baburaja, S. Rajeshkumar, G. Gnanajobitha, C. Malarkodi, M. Sivakavinesan and G. Annadurai, Bioinorganic Chemistry and Applications. 2014, (2014); https://doi.org/10.1155/2014/742346

[29] E.-Y. Ahn, H. Jin, and Y. Park, Materials Science and Engineering: C. 101, 204 (2019); https://doi.org/10.1016/j.msec.2019.03.095

[30] N. Anil and V. Talluri, Rasayan Journal of Chemistry. 14, 2318 (2021); https://doi.org/10.31788/RJC.2021.1446473

[31] M. S. Abdel-Aziz, M. S. Shaheen, A. A. El-Nekeety, and M. A. Abdel-Wahhab, Journal of Saudi Chemical Society. 18, 356 (2014); https://doi.org/10.1016/j.jscs.2013.09.011

[32] R. Mata, J. R. Nakkala, and S. R. Sadras, Colloids and Surfaces B: Biointerfaces. 128, 276 (2015); https://doi.org/10.1016/j.colsurfb.2015.01.052

[33] K. Rajaram, D. C. Aiswarya, and P. Sureshkumar, Materials Letters. 138, 251 (2015); https://doi.org/10.1016/j.matlet.2014.10.017

[34] N. E.-A. El-Naggar, M. H. Hussein, and A. A. El-Sawah, Sci Rep. 7, 1 (2017); https://doi.org/10.1038/s41598-017-11121-3